https://doi.org/10.15407/ujpe64.10.947

R.V. VERBA

Institute of Magnetism Nat. Acad. of Sci. of Ukraine
(36-b, Vernadskogo Blvd., Kyiv 03142, Ukraine; e-mail: verrv@ukr.net)

INTERPLAY OF LINEAR AND NONLINEAR LOCALIZATION MECHANISMS IN SPIN-TORQUE OSCILLATORS WITH A FIELD WELL

The magnetization dynamics in a spin-torque oscillator with nonuniform profile of a static magnetic field creating a field well is studied by analytic calculations and numerical simulations. It is demonstrated that, in the case of sufficiently deep and narrow field well, the linear localization in the field well dominates the nonlinear self-localization, despite a negative nonlinear frequency shift. A change of the localization mechanism results in a qualitatively different dependence of the generation power on the driving current. For the dominant linear localization, the soft generation mode is realized, while, for the nonlinear self-localization, we observe a hard mode of auto-oscillator excitation. Simultaneously, a difference in the profiles of the excited spin-wave mode can become evident and distinguishable in experiments only in the case of a nonsymmetric field well.

Keywords: spin-torque oscillator, spin-wave bullet, localized mode, magnetization dynamics.

1. Introduction

Spin current injected into a ferromagnet creates a torque on its magnetization. Due to the nonconservative nature, this spin-transfer torque can result in the magnetization reversal [1, 2], partial compensation of magnetic losses [3, 4], and excitation of self-sustained magnetization oscillations driven by a dc current [5, 6]. Nanoscale magnetic oscillators, which utilize this effect – spin-torque oscillators (STOs) – are promising for various applications such as compact microwave generators [7, 8], sources of spin waves in magnonics [9, 10], neuromorphic computing [11], etc. Earlier researches utilized the spin-transfer torque of a spin-polarized electric current [1, 5, 6]; the usage of pure spin currents coming from the spin-Hall effect in heavy metals [12] or nonlocal spin current injection [13] enlarges the functionality of STOs.

STOs can demonstrate various types of the nonlinear magnetization dynamics depending on their geometry. In an STO with a nanoscale confined free layer, the spin current excites mostly the lowest quasi-uniform spin-wave mode of the free layer [14] or, in the case of the free layer in a vortex state, the gyrotropic mode of a vortex [15], which is also the lowest among spin-wave modes of a vortex state. In the case of spatially extended free layer (film or nanowire), the dynamics of an STO becomes more complex. It was shown that the injection of a spin current into a large micron-size area of a ferromagnetic film does not allow the excitation of coherent spin waves because of the nonlinear scattering, which redistributes the energy to many spin-wave modes [16]. If the size of the active area, into which the spin current is injected, is reduced down to hundreds of nanometers, the coherent generation becomes possible. Features of the excited spin-wave mode in this case are determined by a nonlinear frequency shift N, which depends on the geometry and static magnetization direction [14]. In the case of positive nonlinear frequency shift, $N > 0$, which is typically realized for the out-of-plane static magnetization direction, the linear spin waves propagating from the active area are excited [17–19]. In contrast, if $N < 0$ (in-plane static magnetization), the excited mode is a nonlinear self-localized spin-wave bullet having characteristic sizes of 100-200 nm [20–22]. Characteristic sizes of the bullet and, consequently, sizes of the STO active area, which supports the coherent generation can be enlarged by the dipolar interaction to the micron-scale in a one-dimensional geometry related to nanowire spin-Hall oscillators [23, 24].

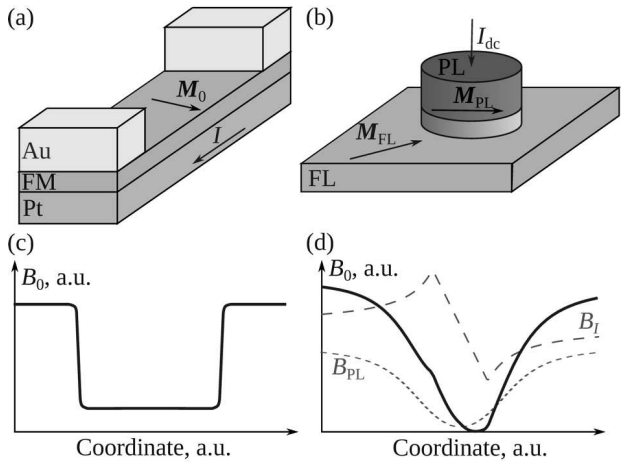

Fig. 1. Sketches of a common nanowire spin-Hall oscillator consisting of a ferromagnetic (FM) – heavy metal (Pt) bilayer with Au electrodes defining the active area between them (*a*), and nanocontact STO with a continuous ferromagnetic film as a free layer (FL) and a nanodot ferromagnetic pinned layer (PL) separated by a dielectric spacer (*b*); (*c, d*) show the corresponding schematic profiles of a static internal magnetic field B_0 (projection of the total magnetic field on the static magnetization direction) in the ferromagnetic layer of SHO (*c*) and in the free layer of nanocontact STO (*d*); in (*d*), dashed lines show separate contributions of the Oersted field B_I and stray fields $B_{\rm PL}$ of the pined layer

This simple picture, however, takes place only in the case of spatially uniform free layers. In a real device, the presence of the Oersted field of a driving current or stray fields from a pinned layer creates a nonuniform energy landscape even in a geometrically uniform magnetic film or nanowire. As an illustration, we show the common geometry of a nanowire spin-Hall oscillator (SHO) [25] and the corresponding profile of a static internal magnetic field affected by the Oersted field of a dc current in Fig. 1, *a, c*. The presence of a field well or field hill in the nanowire depends on the sign of the spin-Hall angle of a heavy metal (as it determines the direction of a current necessary for the spin-wave excitation) and the mutual position of ferromagnetic and heavy metal layers (i.e. which one is on the top). In the case of nanocontact STO with a ferromagnetic film as a free layer (Fig. 1, *b*), the field landscape can be more complex, as it is exemplarily shown in Fig. 1, *d*. In this case, the superposition of the Oersted field of a dc current and the magnetostatic stray fields of the pinned layer can create a complex landscape with a nonsymmetric field well.

Naturally, the presence of a geometric or magnetic nonuniformity in a ferromagnetic free layer affects the STO dynamics and, in particular, may affect the nature of an excited spin-wave mode. Recently, it was shown that the excited spin-wave mode in a nanoconstriction SHO, in which a ferromagnetic layer is patterned, is often a linearly localized mode independent of the static magnetization direction. It is a consequence of the strong nonuniformity of the internal magnetic field and different nonlinear properties of the edge modes compared to the bulk ones [26–28]. In [29], the mode hopping between linearly localized and bullet modes in an SHO with extended active area was found. This means that the excitation thresholds of both these modes are close to each other. Similar hoppings were observed in a constriction-based SHO [27].

In this work, we study the features of localized excitations in an STO within a simple one-dimensional model with a field well. We consider the conditions, when a linear or nonlinear localization mechanism dominates, and how it affects the experimentally measured properties of STO.

2. Model

In this work, the interplay of the linear and nonlinear localization mechanisms is studied within a simple one-dimensional model (e.g., nanowire STO or SHO). We assume that the driving electric current density $J(y)$ and, consequently, spin current density, are constant within the active region of the length $L_{\rm a}$ and are zero outside it (Fig. 2). The nonuniform energy landscape in a ferromagnetic layer is modeled by the rectangular profile of a static internal magnetic field containing a finite-depth field well of the length $L_{\rm w}$. It is described by the spatial dependence of the local ferromagnetic resonance (FMR) frequency $\omega_0(y)$, which is the "fictive" frequency, which a zero-wavenumber spin-wave excitation would have, if the parameters of a sample and the external conditions (e.g., static field) were equal to given local parameters. Obviously, the spatial distribution $\omega_0(y)$ has also rectangular profile with a well (Fig. 2). In a general case, the nonuniformity of a local FMR frequency can be created not only by a nonuniform total external field, but also by a spatial dependence of the magnetic anisotropy, nanowire width or thickness, *etc.* The lengths of the active area and the field well

can be different in the general case, $L_a \neq L_w$. In the most of this work, except for Subsec. 3.3, we consider a symmetric location of the field well and the active area, meaning that their centers coincide, as shown in Fig. 2.

The magnetization dynamics of STO is studied in the framework of the nonlinear Ginzburg–Landau equation, which is derived as an approximation of the Landau–Lifshitz equation accounting for the linear and first nonlinear ($\sim|b|^3$) terms [10, 20, 23]:

$$\frac{\partial b}{\partial t} + (i + \alpha_G)\left(\omega_0(y) - D\frac{\partial^2}{\partial y^2}\right) b + \\ + iN|b|^2 b - \sigma J(y)\left(1 - |b|^2\right) b = 0. \quad (1)$$

Here, $b = b(y,t)$ is the complex amplitude of the dynamic magnetization in the excited spin-wave mode; it is related to the real dynamic magnetization components M_ξ and M_η (orthogonal to each other and to the static magnetization direction) as $b = (M_\xi + i\varepsilon M_\eta)/\sqrt{1+\varepsilon^2}M_s$ with M_s being the saturation magnetization and ε being the ratio of dynamic magnetization components, which describes the ellipticity of the magnetization precession. The magnetic damping is described by the effective damping constant α_G, which could be different from the standard Gilbert constant due to a contribution of the spin pumping into the heavy metal layer (in SHOs) and/or large precession ellipticity. The parameter N describes a nonlinear frequency shift [14]. The coefficient σ is the spin-transfer-torque or spin-Hall efficiency for STO or SHO, respectively, exact expressions for which are not important for our current work and can be found elsewhere [10, 14]. The parameter D describes the spin-wave dispersion and can be achieved from the Taylor expansion of the linear spin wave dispersion relation as $\omega_k \approx \omega_0 + Dk^2 + ...$ [10, 20]. In the case of a soft ferromagnetic film or thin wide nanowire, it is equal to $D = \omega_M\lambda^2(2\omega_H + \omega_M \sin^2\theta_M)/(2\omega_0)$, where $\omega_M = \gamma\mu_0 M_s$, $\omega_H = \gamma B_0$, γ is the gyromagnetic ratio, λ is the exchange length of the ferromagnetic, B_0 is the modulus of the static effective magnetic field, and θ_M is the angle between the static magnetization direction and the film normal. The FMR frequency in this case is equal to $\omega_0 = \left[\omega_H(\omega_H + \omega_M \sin^2\theta_M)\right]^{1/2}$. Formally, it appears that the parameter D is spatially dependent in the presence of a field well. This weak dependence, however, can be easily neglected, by setting the constant D to the value calculated outside the well, since the solution in this region is more sensitive to D, as it determines the radiation losses. Finally, in Eq. (1), we neglect the nonlocal term describing the magnetodipolar interaction (expression including the dipolar term can be found in [23]). It is correct for a sufficiently thin ferromagnetic films and nanowires. Simultaneously, as shown in [23], the dipolar interaction just changes the characteristic length scale, while it does not lead to a qualitatively new behavior of an STO.

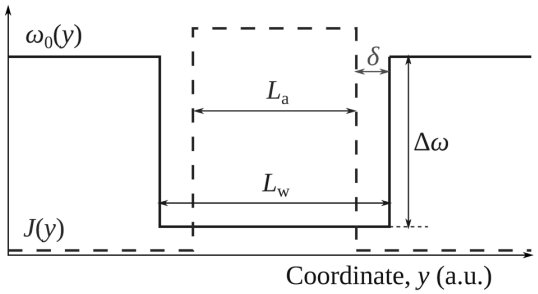

Fig. 2. Studied model of an STO with a field well, showing a spatial distribution of the driving current density $J(y)$ and the local FMR frequency $\omega_0(y)$

It should be noted that the model assumes the well width and depth and a nonlinear frequency shift independent of the amplitude of magnetization precession b. Therefore, it is not directly applicable to the case of wells created by the self-demagnetization fields or excitation of spin-wave modes with anomalous nonlinearity. This more complex case takes place, for example, in constriction-based SHOs [27, 28].

3. Interplay of Localization Mechanisms

3.1. Excitation thresholds of linearly localized and bullet modes

The excitation of a magnetization dynamics in an STO is a threshold process. The generation starts, if the driving current is higher than the threshold value, at which the antidamping spin-transfer torque overcomes total losses (Gilbert damping and radiation losses). Naturally, the mode having the lowest threshold is excited firstly. At large currents, the generation can switch to another regime, e.g., the excitation of higher-order propagating modes [30], second bullet mode [31], multibullet mode [23], mode hopping [32], *etc.* Here, we are not interested in this high-driving-current dynamics and consider only the lowest excited

mode. Therefore, to understand which mode – linear or bullet one – is excited in an STO with a field well, we firsly calculate the excitation threshold for both of them.

A way to calculate the excitation threshold for a linear spin-wave mode is well-known. For this purpose, one needs to find a stationary solution $b(y,t) = b(y)e^{-i\omega t}$ of Eq. (1), neglecting all the nonlinear terms in it [10, 17, 19]. In our case of piecewise constant functions $J(y)$ and $\omega_0(y)$, the solution in each range is a combination of the sine and cosine functions. Applying the boundary conditions of continuity for the dynamic magnetization and its derivative, we get a linear eigenproblem, whose solution yields the generation frequency ω and the threshold current $J_{\rm th}$. Both generation frequency and threshold current are determined from the following implicit equation:

$$k_1\left(k_2 - ik_3\,\tan\left[k_2\delta\right]\right)\tan[k_1 L_{\rm a}/2] = \\ = -ik_2\left(k_3 - ik_2\,\tan\left[k_2\delta\right]\right). \quad (2)$$

Here,

$$k_1 = \sqrt{\left(\omega - \omega_0 + i(\Gamma - \sigma J_{\rm th})\right)/D}, \\ k_2 = \sqrt{\left(\omega - \omega_0 + i\Gamma\right)/D}, \quad (3) \\ k_3 = \sqrt{\left(\omega - \omega_0 - \Delta\omega + i\Gamma\right)/D}$$

are complex spin-wave wavenumbers in the active area, nonactive part of the field well, and the outer region, respectively, $\Gamma = \alpha_G\omega$ is the spin-wave damping rate, $\Delta\omega$ is the depth of the field well, ω_0 is the local FMR frequency within the well, and $\delta = (L_{\rm w} - L_{\rm a})/2$ is the distance between boundaries of the active region and the field well (see Fig. 2). In the case of equal sizes of the active area and the field well, $L_{\rm a} = L_{\rm w}$, Eq. (2) simplifies to the well-known expression [10,19]

$$k_1\,\tan\left[k_1 L_{\rm w}/2\right] = -ik_3. \quad (4)$$

If simultaneously, the well is of infinite depth, which corresponds to a finite-size magnetic dot, then $\mathrm{Im}\left[k_3\right] \to \infty$, and the threshold is determined by Gilbert losses only, $J_{\rm th} = \Gamma/\sigma$.

For the calculation of the bullet excitation threshold, we neglect the presence of a field well. As will be shown below, the nonlinear self-localization dominates over the linear one for relatively wide and/or shallow wells, which this assumption is reasonable for. The method of calculation of the threshold for the bullet mode was described in [20]. The difference from the current work consists in a changed dimensionality of the problem, from two-dimensional to one-dimensional one. In the one-dimensional case, the bullet profile is given by the function $b(y) = b_0\sqrt{2}/\mathrm{ch}[y/l]$, with $l = \sqrt{D/|N|}/b_0$ being the characteristic bullet size, and b_0 being its amplitude. From the condition of energy balance, one can derive the expression for the excitation threshold of a bullet having the amplitude b_0:

$$\frac{\sigma J_{\rm th}}{\alpha_G\omega_0} = \mathrm{cth}\left[\frac{L_{\rm a}}{2l}\right]\left(1 - \frac{2}{3}b_0^2\left(2 + \mathrm{ch}^{-2}\left[\frac{L_{\rm a}}{2l}\right]\right)\right)^{-1}. \quad (5)$$

The real excitation threshold is found as the minimum of expression (5) respective to the bullet amplitude b_0 (we recall that $l = l(b_0)$). The corresponding generation frequency is equal to $\omega = \omega_0 + Nb_0^2$ (we recall that $N < 0$); the bullet size at the threshold is equal to $l = \sqrt{D/|N|}/b_0$ and, typically, is of the order of the active region length $L_{\rm a}$.

3.2. Magnetization dynamics in a symmetric well

For the further consideration, we choose exemplary parameters of STO as follows: $\omega_M = 2\pi \times 30$ GHz, $D = 1.4 \times 10^{-5}$ m^2/s, $\alpha_G = 0.01$, nonlinear frequency shift $N = -2\pi \times 3$ GHz, local FMR frequency is fixed within the well to $\omega_{0,\rm w} = 2\pi \times 6.9$ GHz and is varying outside the well (this is done in order to fix Gilbert losses in the active region, which allows us to distinguish the pure effect of the well presence). These parameters correspond to a permalloy nanowire in the external field of 50 mT.

First, let us look at the simplest case where the sizes of the active region and the field well are equal. The excitation thresholds for the linear and bullet modes calculated by Eqs. (2), (5) are shown in Fig. 3, *a*. In our simplified calculations, the excitation threshold for the bullet mode does not depend on the field well depth and is equal to $J_{\rm th} = 2.2\Gamma/\sigma$. Just as an additional example, we also show the bullet excitation threshold in the case of a twice larger nonlinear frequency shift of $N = -2\pi \times 6$ GHz in Fig. 3, *a*. It is clear that a higher nonlinear frequency shift leads to a decrease of the threshold, as the bullet mode becomes more localized within the active area.

The excitation threshold of the linear mode significantly depends on the field well depth. In the absence of a field well, it is much higher than the bullet

threshold. As the well becomes deeper, the threshold decreases and reaches the value $J_{\rm th} = \Gamma/\sigma$ in the limit of infinitely deep well, i.e., in a confined free layer uniformly pumped by the spin current ($\Delta\omega \to \infty$ at a constant ω_0). The bullet mode cannot reach this minimal threshold value in a confined free layer, and one may expect the excitation of the linear mode in a confined layer of arbitrary sizes. It is, however, not always correct. One should be aware of the excitation of other linear and nonlinear modes. In a large sample (micron-sized in the 2D case; in 1D, it may be larger due to the dipolar interaction), the excitation thresholds for many modes are very close to each other, which results in a chaotic dynamics instead of the coherent generation [16].

From Fig. 3, *a*, one can expect the transition from the bullet mode excitation to the excitation of a linear mode, when the field well becomes deeper than $\Delta\omega = 2\pi \times 0.3\,\text{GHz}$. We simulated the magnetization dynamics by solving numerically the initial equation (1) for two values of the field well depth, below and above this critical value (accounting the nonlinearity and the field well simultaneously). Corresponding stationary profiles of the excited spin-wave mode near the excitation thresholds are shown in Fig. 3, *b*. It is quite hard to distinguish normalized profiles even in simulations and will be completely impossible to do this in experiments. Of course, depending on the values of a nonlinear frequency shift and a field well depth, the characteristic sizes of the bullet and linear modes can become different. However, the localization law is the same. Indeed, the bullet mode $b(y) \sim 1/\text{ch}[y/l]$ is exponentially localized. The linear mode has a lower threshold than bullet ones, when its frequency is below the local FMR frequency outside the well, i.e., when it becomes the evanescent mode. The localization law of this mode outside the well is also exponential and is determined mainly by $b(y) \sim \exp[-\text{Im}[k_3]|y|]$. A small difference within the active region between inverse hyperbolic cosine $1/\text{ch}[y/l]$ and cosine $\cos[k_1 y]$ is too weak to be an evidence of the mode character.

The difference between the bullet and linear modes is pronounced in the dependence of the generation power on the driving current, which is shown in Fig. 3, *c*. For the linear mode, the power at the threshold is vanishingly small and monotonically increases above the threshold (until the nonlinear interaction with other modes becomes important). This

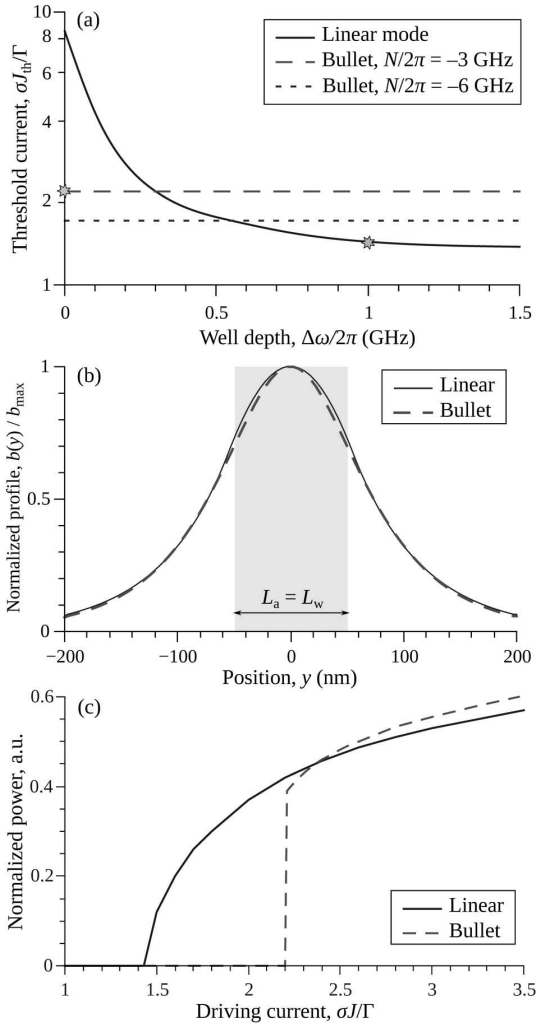

Fig. 3. *a* – calculated excitation threshold of a linearly localized mode as a function of the field well depth and the excitation threshold of the bullet mode at different nonlinear frequency shifts; $L_{\rm a} = L_{\rm w} = 100\,\text{nm}$; stars show points of simulations in panels (*b, c*); *b* – normalized profiles of spin-wave modes close to the threshold for $\Delta\omega = 2\pi \times 1\,\text{GHz}$ (linear mode) and $\Delta\omega = 0$ (bullet); *c* – corresponding dependences of the generation power on the driving current for $\Delta\omega = 2\pi \times 1\,\text{GHz}$ (linear mode) and $\Delta\omega = 0$ (bullet). Panels (*b, c*) are obtained from the numerical solution of Eq. (1)

is the so-called "soft mode" of the excitation of an auto-oscillator. The bullet mode power at the threshold is finite and quite large (hard mode of excitation), because the bullet should have a large amplitude to support its self-localization. These features are the same as for the linear and bullet modes in

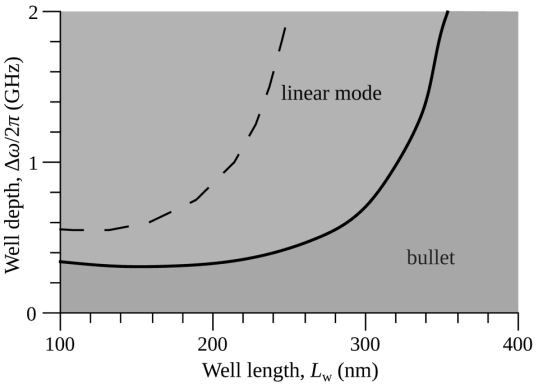

Fig. 4. Phase diagram of STO with the active region of the length $L_a = 100$ nm showing the excitation regions of the bullet and linear modes depending on the length and depth of the filed well; $N = -2\pi \times 3$ GHz. Dashed line show the boundary between the bullet and linear modes in the case of a higher nonlinear frequency shift of $N = -2\pi \times 6$ GHz

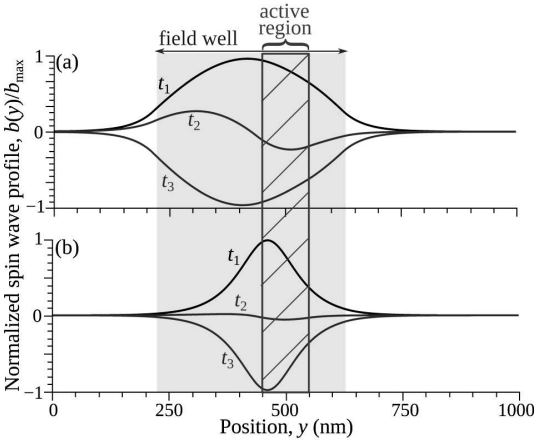

Fig. 5. Example profiles of the linear (a) and bullet (b) modes excited in STO with asymmetric position of the active region respective to the field well. Three instant profiles in each quarter of the oscillation period ($t_1 < t_2 < t_3$) are shown in both panels. Parameters: $L_a = 100$ nm, $L_w = 400$ nm, shift between the well active region centers is 75 nm, well depth $\Delta\omega = 2\pi \times 1$ GHz (a), and $\Delta\omega = 2\pi \times 0.25$ GHz (b)

a uniform ferromagnetic layer [14, 21] and are the main experimentally measured evidence of the nature of the excited spin-wave mode. However, such a simple picture is present only at vanishingly small thermal fluctuations. The sufficient thermal noise could spread the abrupt step in the power dependence, because of the nonstationary hopping between the bullet mode and the generation absence below the real excitation threshold of a bullet [23]. This spreading is more pronounced, if the thresholds of the bullet and linear modes are close to each other, as will happen close to the well depth of 0.3 GHz in our case (see Fig. 3, *a*). In this complex case, only precise time-resolved measurements can distinguish a type of the magnetization dynamics [29].

Above, we considered the case of equal sizes of the active region and the field well, which is a good model for nanowire SHO (see Fig. 1, *a, c*). Figure 4 shows the phase diagram in a more general case of an arbitrary length of the field well, larger than the length of the active region. One can see that, in a sufficiently wide well, the bullet mode is excited in spite of a large well depth. In this case, the localization length of the bullet determined by a nonlinear frequency shift and the active region size becomes less than the field well length. Consequently, the magnetization dynamics does not feel the well and behaves as in a uniform ferromagnetic layer, in which the bullet mode should be excited, if $N < 0$. This characteristic critical well length is, naturally, inversely dependent on the nonlinear frequency shift, because the higher values of the nonlinear shift make the bullet mode more localized. Thus, we can conclude that the significantly narrow and deep field wells support the linearly localized mode formation. Otherwise, the bullet mode is excited.

3.3. Spin-wave profiles in a nonsymmetric well

In this section, we briefly discuss how the asymmetry of positions of the active region and the field well affects the STO dynamics. Such case of nonsymmetric well can appear in nanocontact STOs, as shown in Fig. 1, *d*. We model the asymmetry by a shift of the field well center respective to the active region center, while both still are of a rectangular profile. Simulations show that the asymmetry does not lead to a qualitative change of the STO phase diagram and the generation power dependence. The sufficiently narrow deep well supports the excitation of the linear mode in a soft excitation mode. Otherwise, the hard mode of the bullet excitation takes place. Simultaneously, the difference in spin-wave profiles could be substantial.

In Fig. 5, we show the profiles of the linearly localized and bullet modes in a nonsymmetric well. One can see that the presence of the well leads to a shift of

the bullet mode from the center of the active area toward to the center of the well (Fig. 5, *b*). This happens because "tails" of the bullet feel the boundaries of the well. This shift is more pronounced in a deeper well, if it stills support the bullet formation. The bullet has a standing-mode character, and the magnetization at different points oscillates with approximately the same phase, as it does in the case of a symmetric well or in the absence of a well. The effect of an asymmetry on a linearly localized mode is more pronounced. This mode becomes nonstanding, i.e., the magnetization oscillates not in the same phase in all the sample. The position of a maximum of the instant spin-wave profile changes during the oscillation period. Moreover, the profile varies from one having one maximum to that with two maxima, as shown in Fig. 5, *b* (number of maxima may differ depending on the well size). This complex dynamics is a result of the excitation of quasipropagating spin waves by the active region and its quantization in the well.

We believe that such a transition from a nonlinear to linear localization of the excited mode was observed in [33], but was incorrectly treated. In [33], it was stated that depending on external conditions, the one- or two-bullet mode, which are called *s*- or *p*-like bullets, is excited at the threshold. However, there is no other experimental or theoretical work, where the two-bullet solution (or the second bullet mode) was observed at the threshold. The second bullet mode always appears at a some higher threshold after the single-bullet mode is excited [23, 31]. We do not see any cause for why the two-bullet mode could be more energy-favorable than a single-bullet one. Indeed, the formation of the two-bullet mode always increases the exchange energy comparing to a single-bullet one. The nonuniformity of the energy landscape or bias current leads only to a shift of the single-bullet mode at the threshold, as is shown in this work and in [23], respectively. Simultaneously, the qualitative features of the mode observed in [33] are the same, as we found in a nonsymmetric well. Both the experiment and micromagnetic simulations in [33] showed that the mode, which was interpreted as a "*p*-like" soliton, has quasipropagating character with a variation in the number of instant maxima from one to two during the oscillation period. The nanocontact STO studied in [33] is similar to one shown in Fig. 1, *b*, which demonstrates a complex nonsymmetric magnetic field landscape. Therefore, we can state that the observed excitation in that work was a linear mode localized in a field well.

4. Conclusions

In this work, the magnetization dynamics in a spin-torque oscillator with a nonuniform profile of the static magnetic field creating a field well has been studied. It is demonstrated that the presence of the field well can change the nature of the excited spin-wave mode. A shallow and/or wide well does not affect much the magnetization dynamics, and the bullet mode is excited in an STO having a negative nonlinear frequency shift, as it happens in the absence of a well. In contrast, if the well is sufficiently deep and narrow, the linear localization mechanism dominates over the nonlinear self-localization, despite a negative nonlinear frequency shift, and a linear localized spin-wave mode is excited. A change of the localization mechanism results in a qualitatively different dependence of the generation power on the driving current. For the dominant linear localization, the soft generation mode is realized, while we observe the hard mode of auto-generator excitation for the nonlinear self-localization. Simultaneously, in the case of a symmetric position of the well and the active region, the difference in the profiles of the linear and bullet spin-wave modes is weak. They have the exponential localization outside the well and the difference in the mode profiles within the active region is hardly distinguishable in experiment. But, in a nonsymmetric well, the profiles of the linear and bullet modes can differ drastically. While the bullet mode remains of a standing-mode character, the linear mode could acquire a quasipropagating character, which can be easily detected by a spatial mapping of the magnetization dynamics.

The work was sponsored by the Ministry of Education and Science of Ukraine (grant No. 0118U004007).

1. J.A. Katine, F.J. Albert, R.A. Buhrman, E.B. Myers, D.C. Ralph. Current-driven magnetization reversal and spin-wave excitations in Co/Cu/Co pillars, *Phys. Rev. Lett.* **84**, 3149 (2000).
2. R. Ramaswamy, J.M. Lee, K. Cai, H. Yang. Recent advances in spin-orbit torques: Moving towards device applications. *Appl. Phys. Rev.* **5**, 031107 (2018).
3. K. Ando, S. Takahashi, K. Harii, K. Sasage, J. Ieda, S. Maekawa, E. Saitoh. Electric manipulation of spin re-

laxation using the spin Hall effect. *Phys. Rev. Lett.* **101**, 036601 (2008).
4. A. Hamadeh, O. d'Allivy Kelly, C. Hahn, H. Meley, R. Bernard, A.H. Molpeceres, V.V. Naletov, M. Viret, A. Anane, V. Cros, S.O. Demokritov, J.L. Prieto, M. Muñoz, G. de Loubens, O. Klein. Full control of the spin-wave damping in a magnetic insulator using spin-orbit torque. *Phys. Rev. Lett.* **113**, 197203 (2014).
5. S.I. Kiselev, J.C. Sankey, I.N. Krivorotov, N.C. Emley, R.J. Schoelkopf, R.A. Buhrman, D.C. Ralph. Microwave oscillations of a nanomagnet driven by a spin-polarized current. *Nature* **425**, 380 (2003).
6. W.H. Rippard, M.R. Pufall, S. Kaka, S.E. Russek, T.J. Silva. Direct-current induced dynamics in $Co_{90}Fe_{10}$/ $Ni_{80}Fe_{20}$ point contacts. *Phys. Rev. Lett.* **92**, 027201 (2004).
7. O. Prokopenko, E. Bankowski, T. Meitzler, V. Tiberkevich, A. Slavin. Spin-torque nano-oscillator as a microwave signal source. *IEEE Magn. Lett.* **2**, 3000104 (2011).
8. S. Tsunegi, H. Kubota, K. Yakushiji, M. Konoto, S. Tamaru, A. Fukushima, H. Arai, H. Imamura, E. Grimaldi, R. Lebrun, J. Grollier, V. Cros, S. Yuasa. High emission power and Q factor in spin torque vortex oscillator consisting of FeB free layer. *Appl. Phys. Express* **7**, 063009 (2014).
9. V.E. Demidov, S. Urazhdin, R. Liu, B. Divinskiy, A. Telegin, S.O. Demokritov. Excitation of coherent propagating spin waves by pure spin currents. *Nature Commun.* **7**, 10446 (2016).
10. A. Giordano, R. Verba, R. Zivieri, A. Laudani, V. Puliafito, G. Gubbiotti, R. Tomasello, G. Siracusano, B. Azzerboni, M. Carpentieri, A. Slavin, G. Finocchio. Spin-Hall nano-oscillator with oblique magnetization and Dzyaloshinskii–Moriya interaction as generator of skyrmions and nonreciprocal spin-waves. *Sci. Rep.* **6**, 36020 (2016).
11. J. Torrejon, M. Riou, F.A. Araujo, S. Tsunegi, G. Khalsa, D. Querlioz, P. Bortolotti, V. Cros, K. Yakushiji, A. Fukushima, H. Kubota, S. Yuasa, M.D. Stiles, J. Grollier. Neuromorphic computing with nanoscale spintronic oscillators. *Nature* **547**, 428 (2017).
12. V.E. Demidov, S. Urazhdin, H. Ulrichs, V. Tiberkevich, A. Slavin, D. Baither, G. Schmitz, S.O. Demokritov. Magnetic nano-oscillator driven by pure spin current,. *Nat. Mater.* **11**, 1028 (2012).
13. V.E. Demidov, S. Urazhdin, A. Zholud, A.V. Sadovnikov, A.N. Slavin, S.O. Demokritov. Spin-current nano-oscillator based on nonlocal spin injection. *Sci. Rep.* **5**, 8578 (2015).
14. A. Slavin, V. Tiberkevich. Nonlinear auto-oscillator theory of microwave generation by spin-polarized current. *IEEE Trans. Magn.* **45**, 1875 (2009).
15. V.S. Pribiag, I.N. Krivorotov, G.D. Fuchs, P.M. Braganca, O. Ozatay, J.C. Sankey, D.C. Ralph, R.A. Buhrman. Magnetic vortex oscillator driven by d.c. spin-polarized current. *Nature Phys.* **3**, 498 (2007).
16. V.E. Demidov, S. Urazhdin, E.R.J. Edwards, M.D. Stiles, R.D. McMichael, S.O. Demokritov. Control of magnetic fluctuations by spin current. *Phys. Rev. Lett.* **107**, 107204 (2011).
17. J. Slonczewski. Excitation of spin waves by an electric current. *J. Magn. Magn. Mater.* **195**, L261 (1999).
18. M.A. Hoefer, M.J. Ablowitz, B. Ilan, M.R. Pufall, T.J. Silva. Theory of magnetodynamics induced by spin torque in perpendicularly magnetized thin films. *Phys. Rev. Lett.* **95**, 267206 (2005).
19. G. Consolo, L. Lopez-Diaz, B. Azzerboni, I. Krivorotov, V. Tiberkevich, A. Slavin. Excitation of spin waves by a current-driven magnetic nanocontact in a perpendicularly magnetized waveguide. *Phys. Rev. B* **88**, 014417 (2013).
20. A. Slavin, V. Tiberkevich. Spin wave mode excited by spin-polarized current in a magnetic nanocontact is a standing self-localized wave bullet. *Phys. Rev. Lett.* **95**, 237201 (2005).
21. G. Consolo, B. Azzerboni, G. Gerhart, G.A. Melkov, V. Tiberkevich, A.N. Slavin. Excitation of self-localized spin-wave bullets by spin-polarized current in in-plane magnetized magnetic nanocontacts: A micromagnetic study. *Phys. Rev. B* **76**, 144410 (2007).
22. S. Bonetti, V. Tiberkevich, G. Consolo, G. Finocchio, P. Muduli, F. Mancoff, A. Slavin, J. Åkerman. Experimental evidence of self-localized and propagating spin wave modes in obliquely magnetized current-driven nanocontacts. *Phys. Rev. Lett.* **105**, 217204 (2010).
23. L. Yang, R. Verba, V. Tiberkevich, T. Schneider, A. Smith, Z. Duan, B. Youngblood, K. Lenz, J. Lindner, A.N. Slavin, I.N. Krivorotov. Reduction of phase noise in nanowire spin orbit torque oscillators. *Sci. Rep.* **5**, 16942 (2015).
24. K. Wagner, A. Smith, T. Hache, J.-R. Chen, L. Yang, E. Montoya, K. Schultheiss, J. Lindner, J. Fassbender, I. Krivorotov, H. Schultheiss. Injection locking of multiple auto-oscillation modes in a tapered nanowire spin Hall oscillator. *Sci. Rep.* **8**, 16040 (2018).
25. Z. Duan, A. Smith, L. Yang, B. Youngblood, J. Lindner, V.E. Demidov, S.O. Demokritov, I.N. Krivorotov. Nanowire spin torque oscillator driven by spin-orbit torques. *Nature Commun.* **5**, 5616 (2014).
26. M. Dvornik, A.A. Awad, J. Åkerman. Origin of magnetization auto-oscillations in constriction-based spin Hall nano-oscillators. *Phys. Rev. Applied* **9**, 014017 (2018).
27. H. Mazraati, S.R. Etesami, S.A.H. Banuazizi, S. Chung, A. Houshang, A.A. Awad, M. Dvornik, J. Åkerman. Auto-oscillating spin-wave modes of constriction-based spin Hall nano-oscillators in weak in-plane fields. *Phys. Rev. Applied* **10**, 054017 (2018).
28. M. Dvornik, J. Åkerman. Anomalous nonlinearity of the magnonic edge mode. arXiv:1804.01585 [cond-mat.mes-hall].
29. B. Divinskiy, V.E. Demidov, S. Urazhdin, R. Freeman, A.B. Rinkevich, S.O. Demokritov. Controllable excitation of quasi-linear and bullet modes in a spin-Hall nano-oscillator. *Appl. Phys. Lett.* **114**, 042403 (2019).

30. A. Houshang, R. Khymyn, H. Fulara, A. Gangwar, M. Haidar, S.R. Etesami, R. Ferreira, P.P. Freitas, M. Dvornik, R.K. Dumas, J. Åkerman. Spin transfer torque driven higher-order propagating spin waves in nano-contact magnetic tunnel junctions. *Nature Commun.* **9**, 4374 (2018).

31. H. Ulrichs, V.E. Demidov, S.O. Demokritov. Micromagnetic study of auto-oscillation modes in spin-Hall nano-oscillators. *Appl. Phys. Lett.* **104**, 042407 (2014).

32. G. Consolo, G. Finocchio, G. Siracusano, S. Bonetti, A. Eklund, J. Åkerman, B. Azzerboni. Non-stationary excitation of two localized spin-wave modes in a nano-contact spin torque oscillator. *J. Appl. Phys.* **114**, 153906 (2013).

33. S. Bonetti, R. Kukreja, Z. Chen, F. Macià, J.M. Hernàndez, A. Eklund, D. Backes, J. Frisch, J. Katine, G. Malm, S. Urazhdin, A. D. Kent, J. Stöhr, H. Ohldag, H.A. Dürr. Direct observation and imaging of a spin-wave soliton with *p*-like symmetry. *Nature Commun.* **6**, 8889 (2015).

Received 18.04.19

Р.В. Верба

КОНКУРЕНЦІЯ ЛІНІЙНОГО
ТА НЕЛІНІЙНОГО МЕХАНІЗМІВ
ЛОКАЛІЗАЦІЇ В СПІН-ТОРК ОСЦИЛЯТОРАХ
ЗА НАЯВНОСТІ ПОТЕНЦІАЛЬНОЇ ЯМИ

Р е з ю м е

Аналітично та числовими методами досліджується динаміка намагніченості у спін-торк осциляторах з неоднорідним профілем статичного магнітного поля, який утворює потенціальну яму. Продемонстровано, що у випадку достатньо глибокої та вузької потенціальної ями лінійний механізм локалізації домінує над нелінійною самолокалізацією, незважаючи на від'ємний нелінійний зсув частоти спінових хвиль. Зміна механізму локалізації відображається у якісно різних залежностях потужності генерації від струму накачки – у випадку лінійної локалізації реалізується м'який режим збудження автогенератора, тоді як у випадку нелінійної самолокалізації спостерігається жорсткий режим збудження. При цьому різниця профілів збуджених спін-хвильових мод стає помітною та такою, що може бути експериментально виміряною, лише у випадку несиметричного положення потенціальної ями.